



# Investigation of physico-chemical and optoelectronic properties of MoTe<sub>2</sub> FET

<sup>1</sup>Kamoladdin Saidov, <sup>2</sup>Shavkat Mamatkulov, <sup>3</sup>Khakimjan Butanov, <sup>4</sup>Van Ngoc Huynh and <sup>5</sup>Olim Ruzimuradov

<sup>1,2,3,5</sup>Institute of Material Science, Academy of Sciences of the Republic of Uzbekistan, Uzbekistan.

<sup>4</sup>Department of Biotechnology and Biomedicine Section for Protein Science and Biotherapeutics, Technical University of Denmark

<sup>5</sup>Department of Natural and Mathematic Sciences, Turin Polytechnic University in Tashkent, Uzbekistan.

<sup>1</sup>Email: k.saidov@skku.edu

**Abstract**– In this article, we explore the nature of photocurrent generation mechanisms in MoTe<sub>2</sub> based field effect transistors (FETs) by using gate and bias-dependent photocurrent measurements. Our results reveal that the photocurrent signals at MoTe<sub>2</sub>-electrode junctions are mainly attributed to the gain photoconductor effect in the off-state and on-state. The photocurrent peak is distinguished from conventional MoTe<sub>2</sub> FETs, which show a continuous increase in photocurrent with back-gate voltage. These results offer significant insight and further enhance the understanding of the directional-dependent absorption of MoTe<sub>2</sub> crystals.

**Key words**– Photodetector, field-effect transistor, MoTe<sub>2</sub>, photocurrent gate

## I INTRODUCTION

While fossil fuels have been integral in the development of most industrial nations, there are a few realities of using them that society needs to come to terms with. There are many arguments in favor of society's need for renewable energy. The isolation of graphene in 2004, rapidly followed by the discovery of its amazing properties, has generated an intense research effort on layered 2D (two-dimensional) materials[1]. Low dimensional materials have exhibited exotic physical properties. Among them, TMDs (transition-metal dichalcogenides) layered semiconducting materials such as MoS<sub>2</sub>, MoSe<sub>2</sub>, WS<sub>2</sub>, WSe<sub>2</sub> and MoTe<sub>2</sub> have attracted a great attention due to the possibility for a candidate material for post-Si era. Even in their single layer form, semiconducting TMDs materials have demonstrated efficient light absorption, enabling large responsivity in photodetectors. Therefore, semiconducting layered TMDs materials are strong candidates for optoelectronic applications, especially for photodetection. The rectification nature of the source-drain current with the back gate voltage reveals the presence of a stronger Schottky barrier at the MoTe<sub>2</sub>-metal contact[2].

For electronic applications, semiconducting 2D TMDs materials benefit from sizable mobilities and large on/off ratios, due to the large modulation achievable via the gate field-effect. However, the absence of an intrinsic bandgap in graphene has hindered its development for use in logic circuits in the modern semiconductor industry, stimulating scientific and engineering progress on its derivatives and other TMDs layered nanomaterials. TMDs with the common formula MX<sub>2</sub>, where M stands for a transition metal from group IV-VII (M = Mo, W, Nb, Re, and so on) and X is a chalcogen element (X = S, Se, Te), form a well-known class of layered composite materials. In these layered materials, a hexagonally packed layer of M atoms is sandwiched between two layers of X atoms, and the triple layers stack together via weak van der Waals forces, which facilitate cleavage of the bulk crystals to form individual 2D flakes along each triplet of layered structures. The lack of covalent bonds between adjacent triple layers renders these 2D TMD flakes free of dangling bonds, thus creating chemical stability and low carrier scattering on their surfaces. These layered TMD structures lead to high anisotropy in their electrical properties[3-4]. Photodetectors are a key component of many devices we use in our daily life. From imaging to optical communications, we have photodetectors to convert the information stored in light into electrical signals that can be processed by standard electronics. Silicon photodetectors are readily integrated in semiconducting 2D materials technology. Bulk Silicon photodetectors suffer from the limitations of silicon as a light-absorbing material. Its indirect bandgap of about 1.07 eV limits absorption to the visible and near-infrared part of the electromagnetic spectrum and reduces its efficiency. To achieve sizable responsivities, photodetectors based on bulk silicon rely on a thick channel, making the photodetector fully opaque. In the photoconductive effect, photon absorption generates extra free carriers, reducing the elec-

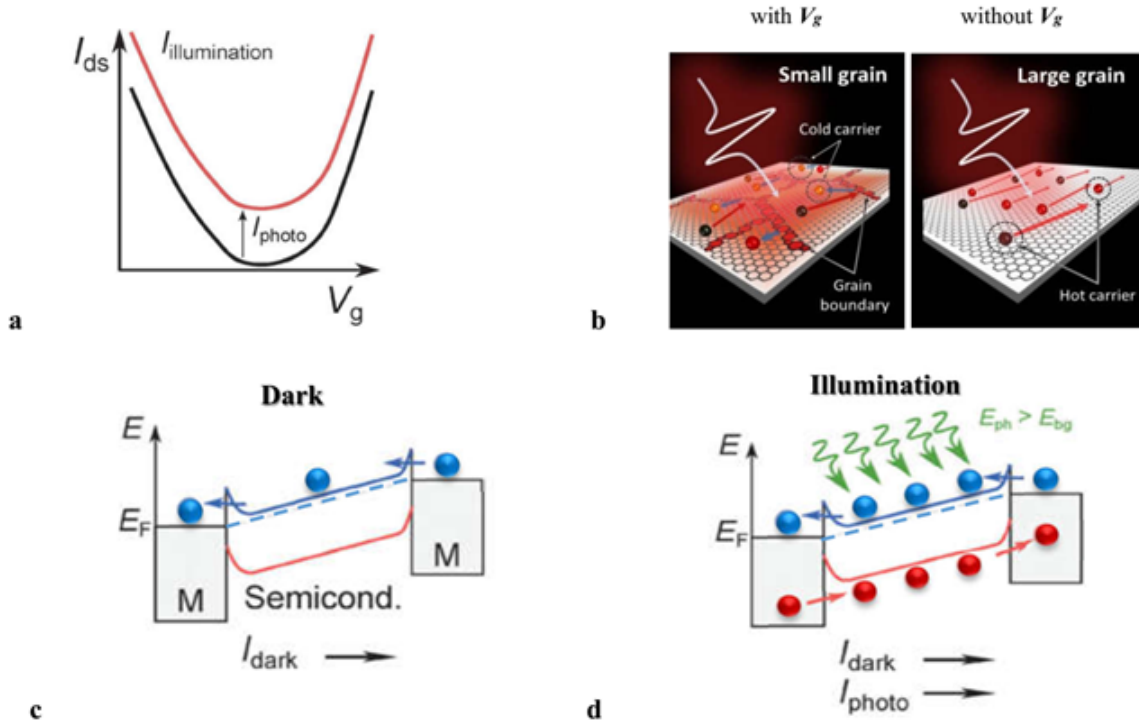


**Fig. 1:** Schematic of the photoconductive effect. a)  $I_{ds}$ - $V_g$  traces in the dark (solid black line) and under illumination (solid red line). Illumination results in an increase in the conductivity (vertical shift) and a positive photocurrent across the entire gate voltage range, b) a schematic representation of a phototransistor consisting of by the gate doping and without. c) Band alignment for a semiconductor channel contacted with two metals (M) under an external bias without illumination. A small current flows through the device ( $I_{dark}$ ). d) Band alignment under illumination with photons of energy ( $E_{ph}$ ) higher than the bandgap ( $E_{bg}$ ). The absorption of photons generates electron-hole pairs that are separated by the external applied bias, generating a photocurrent ( $I_{photo}$ ) which adds to  $I_{dark}$

trical resistance of the semiconductor. Without illumination and under an applied bias ( $V_{ds}$ ), a small source-drain current can flow ( $I_{dark}$ ). Under illumination, the absorption of photons with energy higher than the bandgap ( $E_{ph} > E_{bg}$ ) generates e-h pairs which are separated by the applied  $V_{ds}$ . The photogenerated free electrons and holes drift in opposite directions towards the metal leads, resulting in a net increase in the current ( $I_{photo}$ ).

This photogenerated current adds to the dark current, reducing the resistance of the device, as depicted in Figure 1. It is instructive to consider the case of a large difference between the electron and hole mobilities, resulting in a large difference in the electron/hole transit time ( $\tau_{transit}$ )

$$\tau_{transit} = \frac{L^2}{\mu V_{ds}}$$

where  $L$  is the length of the transistor channel,  $\mu$  the charge carrier mobility and  $V_{ds}$  the source-drain bias[5]. If the hole mobility is much lower than the electron mobility, the photogenerated electrons can cross the channel much faster

than the photogenerated holes. Until recombination or hole extraction, many electrons can participate in the photocurrent, leading to the photoconductive gain ( $G$ ). Effectively, this means that more electrons can be extracted from a single photon. The photoconductive gain is the ratio of the photogenerated carrier lifetime ( $\tau_{photocarriers}$ ) and the transit time[6].

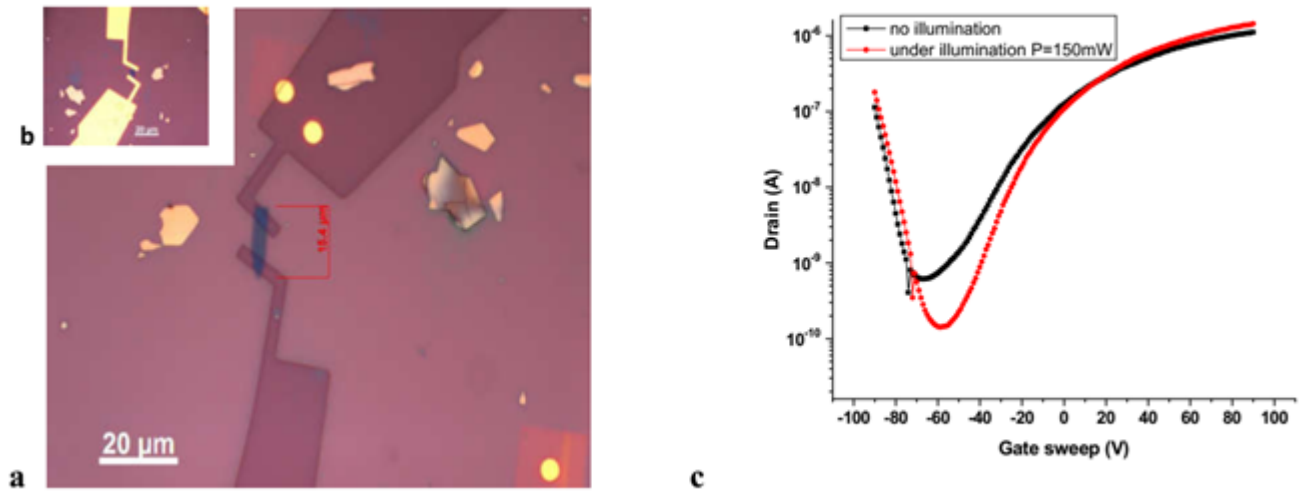
$$G = \frac{\tau_{photocarriers}}{\tau_{transit}} = \frac{\tau_{photocarriers} \mu V}{L^2}$$

This effect is of particular importance for nanostructured materials, like two dimensional semiconductors, where the large surface and reduced screening play a major role in the electrical properties. Hence, large ( $\tau_{photocarriers}$ ) and a large mismatch in the electron/hole mobility yield large  $G$ .

## II RESULTS AND DISCUSSION

We are proposed a new structure of memory devices for n/p type field-effect transistors (FETs) based on few and mono layer of TMD materials. Figure 2 shows the schematic

Transition metals-M		Chalcogens -X <sub>2</sub>		
Group	Metals	-S <sub>2</sub>	-Se <sub>2</sub>	-Te <sub>2</sub>
IV	Zr	Semiconductor; bulk: 1.75 eV	Semiconductor	Semiconductor
	Hf	Semi-insulator	Semiconductor; bulk 1.15 eV	Semiconductor
V	V	Metal	Metal	Metal
	Nb	1T phase; Metal; superconducting	Metal; Superconducting	Metal
	Ta	Metal; Superconducting	Metal; Superconducting	Metal
VI	Mo	Semiconductor; 1L: 1.8 eV; bulk: 1.3 eV	Semiconductor; 1L: 1.5 eV; bulk: 1.1 eV	Semiconductor; 1L: 1.1 eV; bulk: 0.6 eV
	W	Semiconductor; 1L: 2.1 eV; bulk: 1.4 eV	Semiconductor; 1L: 1.7 eV; bulk: 1.2 eV	Semiconductor; 1L: 1.1 eV
X	Pd	Semiconductor	Semiconductor	Metal; superconducting
	Pt	Semiconductor; bulk: 0.7 eV	Semiconductor; bulk: 0.1 eV	Metal

**TABLE 1:** ELECTRONIC PROPERTIES OF DIFFERENT LAYERED TMDS


**Fig. 2:** a) schematic structure of the fabrication of MoTe<sub>2</sub> onto a 300 nm SiO<sub>2</sub> substrate (optical image of the device after the electron-beam lithography processes), b) optical image of the MoTe<sub>2</sub> junction with few-layers (after the electron beam-metal deposition) and c) the current vs. gate voltage and under illumination characteristics at various V<sub>bias</sub>.

structure of the fabrication of MoTe<sub>2</sub> and optical image of the MoTe<sub>2</sub> junction with few-layer film deposited onto a 300 nm Si/SiO<sub>2</sub> substrate. We have focused on the p-type on SiO<sub>2</sub> MoTe<sub>2</sub> FET device measurements.

P- and n-type on SiO<sub>2</sub> MoTe<sub>2</sub> FET devices will be determined from current-voltage (I V) measurements of FET. I V characteristics are measured using one of Model 4200-SCS's Source Measure Units (SMUs), which can source and measure both current and voltage. It indicates that the lower

gate voltage can lead to a higher Schottky barrier[7] height between metal (Au/Ti) and MoTe<sub>2</sub>. Figure 2c shows the current vs. gate voltage characteristics of various V<sub>bias</sub>. The MoTe<sub>2</sub> is the core of FET devices[8]. In order to fundamentally understand the physics of the metal junction, a theoretical model is established[9]. The electrical performance of our device is mainly dependent on the metal junction. In this case, the lateral transport is the dominant factor, suggesting that the resistance of this uniform junction. Therefore, the

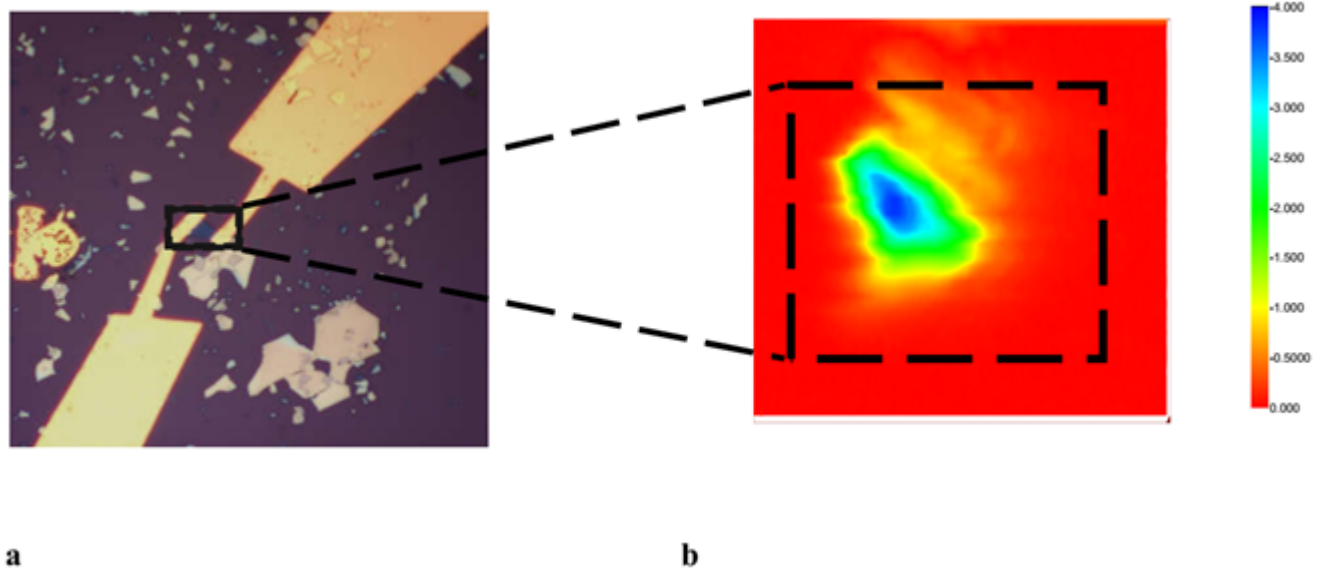


**Fig. 3:** a) optical image of  $\text{MoTe}_2$  FET. b) Photo current map of the transistor at  $V_{sd} = 500\text{mV}$  and  $V_{bg} = 30\text{V}$  with laser power  $150\text{ mW/cm}^2$ . Black dashed line outlines the region of  $\text{MoTe}_2$ .

junction could also be regarded as an artificial thin film FET. These two resistors are included to consider the resistances of  $\text{MoTe}_2$  between the junction and source/drain electrodes. Here  $\text{MoTe}_2$  is considered as a thin bulk material, and the drop of electric potential in electrode is ignored since it has only several layers[10]. We now discuss the optical response of the transistor. Fig. 3(b) shows the scanning photocurrent mapping of an area (Fig. 3(b)) ( $8 \times 5\ \mu\text{m}$ ) around the  $\text{MoTe}_2$  structures at  $V_{bg} = 30\text{V}$ . Here,  $\text{MoTe}_2$  was biased with  $V_{sd} = 500\text{mV}$  and the photo current was measured through the channel.

We observe a higher photocurrent at  $\text{MoTe}_2$  (blue region in Fig. 3(b)) as compared to only the  $\text{MoTe}_2$  part. The values of photo induced currents are  $60\text{ nA}$ ,  $10\text{ nA}$ , and  $1\text{ nA}$  at  $\text{MoTe}_2$  and  $\text{SiO}_2$  substrate interface, respectively. With laser on, the current increases by 15–20 times (at  $V_{sd} = 500\text{mV}$ ). When the  $\text{MoTe}_2$  is illuminated, the photo-generated electrons and holes in photo-active  $\text{MoTe}_2$  are easily separated by highly conductive interface due to the applied electric field ( $V_{sd}$ ) resulting in enhanced current[11]. When the laser is turned on, the photo carriers are generated and the built-in electric field at the  $\text{MoTe}_2$ - $\text{SiO}_2$  interface due to the Schottky barrier separates the carriers apart, resulting in the short circuit current. In order to modulate the Schottky barrier height significantly, we change the laser power and more number of photo carriers are generated which are separated by the applied source drain bias and the photocurrent increases sub-linearly with the laser power. The Seebeck coefficient, making it a promising material for thermal energy harvesting[12-14].

In this article, we can achieve the current state in photodetection with layered semiconducting materials photodetectors should be based on TMDCs, especially  $\text{MoTe}_2$  show large responsivity coupled to slow response times, indicating that these materials can be suitable for sensitive applications in the visible and when time response is not important. We also remind that the photocurrent due to the photovoltaic effect in these  $\text{MoTe}_2$  diodes is approximately larger currents observed at the contacts of a monolayer  $\text{MoTe}_2$  field-effect transistor[15].

### III METHODS

The bulk  $\text{MoTe}_2$  was purchased from 2D semiconductors. A few layers of the material were deposited onto a substrate by using the mechanical exfoliation method. An optical microscope (OM) image of the multipurpose  $\text{MoTe}_2$  device fabricated. Since our  $\text{MoTe}_2$  is also prepared with mechanical exfoliation, for the above reason, we choose a flake with the thickness of  $17\text{ nm}$  ( $21$  atomic layers), to minimize the effect by the interface traps on the photoresponse of  $\text{MoTe}_2$ , and to maximize the effect of the midgap states in the experiment[12]. Electrodes were patterned using electron-beam lithography, and  $\text{Cr/Au}$  ( $5/30\text{ nm}$ ),  $\text{Au}$  ( $30\text{ nm}$ ) were deposited for  $\text{MoTe}_2$  contacts, respectively, by electron beam evaporator system.

## IV CONCLUSIONS

In summary, the van der Waals forces between the two different TMDs result in a band offset that gives rise to the directional electrical conductance that is governed by thermionic emission. The effective bandgap of the MoTe<sub>2</sub> is narrow enough (approximately 0.8 eV) to facilitate interband tunneling of carriers under reverse bias. However, tunneling characteristics were not observed. Therefore, the device parameters were controlled to realize tunneling current. In this study, the contact resistance was lowered and the depletion region width was reduced by changing the metal electrode. In our study, a peak-to-valley ratio of 4.8 was determined. This value is comparable to that of well-established Si tunneling diodes. By adopting atomically thin s-TMDs, the application of inorganic solid state electronic devices has been expanded to the flexible regime.

## REFERENCES

- [1] K. S. Novoselov, A. K. Geim, S. V. Morozov, D. Jiang, Y. Zhang, S. V. Dubonos, I. V. Grigorieva and A. A. Firsov, “Electric field effect in atomically thin carbon films”, *Science*, 2004, 306, 666–669.
- [2] A. Pezeshki, S. H. Shokouh, T. Nazari, K. Oh, and S. Im, “Electric and Photovoltaic Behavior of a Few-Layer -MoTe<sub>2</sub>/MoS<sub>2</sub> Dichalcogenide Heterojunction”, *Adv. Mater.* 2016, 28, 3216–3222
- [3] K. S. Novoselov, A. K. Geim, S. V. Morozov, D. Jiang, M. I. Katsnelson, I. V. Grigorieva, S. V. Dubonos and A. A. Firsov, “Two-dimensional gas of massless Dirac fermions in grapheme”, *Nature*, 2005, 438, 197–200.
- [4] Y. F. Lin, Y. Xu, S. L. Li, M. Yamamoto, A. A. Ferreira, W. Li, H. Sun, S. Nakahara and K. Tsukagoshi “Ambipolar MoTe<sub>2</sub> Transistors and Their Applications in Logic Circuits”, *Adv. Mater.* 2014, 26, 3263–3269.
- [5] K. S. Novoselov, Z. Jiang, Y. Zhang, S. V. Morozov, H. L. Stormer, U. Zeitler, J. C. Maan, G. S. Boebinger, P. Kim and A. K. Geim, “Room-Temperature Quantum Hall Effect in Graphene”, *Science*, 2007, 315, 1379.
- [6] B. Saleh and M. Teich, “Fundamentals of photonics” (Book), Wiley, 1991.
- [7] N. Dhar, T. H. Chowdhury, m. A. Islam, N. A. Khan, M. J. Rashid, M. M. Alam, Z. A. Alothman, K. Sopian, N. Amin “Effect of n-type transition metal dichalcogenide molybdenum telluride (n-MoTe<sub>2</sub>) in back contact interface of cadmium telluride solar cells from numerical analysis”, *Chalcogenide Letters* Vol. 11, No. 6, June 2014, p. 271 - 279
- [8] F. Xia, T. Mueller, Y.-m. Lin, A. Valdes-Garcia and P. Avouris, “Ultrafast grafene photodetector”, *Nat. Nanotechnol.*, 2009, 4, 839–843.
- [9] S. Song, D. H. Keum, S. Cho, D. Perello, Y. Kim, and Y. H. Lee, “Room Temperature Semiconductor-Metal Transition of MoTe<sub>2</sub> Thin Films Engineered by Strain”, *Nano Lett.* 2016, 16, 188-193
- [10] Sh. Nakaharai, M. Yamamoto, K. Ueno, and K. Tsukagoshi, “Carrier Polarity Control in MoTe<sub>2</sub> Schottky Junctions Based on Weak Fermi-Level Pinning”, *ACS Appl. Mater. Interfaces* 2016, 8, 14732-14739
- [11] L. Wang, I. Meric, P. Y. Huang, Q. Gao, Y. Gao, H. Tran, T. Taniguchi, K. Watanabe, L. M. Campos, D. A. Muller, J. Guo, P. Kim, J. Hone, K. L. Shepard and C. R. Dean, “One-Dimensional Electrical Contact to a Two-Dimensional Material”, *Science*, 2013, 342, 614–617.
- [12] C. Ruppert, O. Burak Aslan, Tony F. Heinz, “Optical Properties and Band Gap of Single- and Few-Layer MoTe<sub>2</sub> Crystals” *Nano Lett.* 2014, 14, 6231-6236
- [13] M. Kuiri, B. Chakraborty, A. Paul, S. Das, A. K. Sood, A. Das, “Enhancing photoresponsivity using MoTe<sub>2</sub>-graphene vertical heterostructures”, *Appl. Phys. Lett.* 108, 063506 (2016)
- [14] A. Conan, G. Goreaux, M. Zoeter, *J. Phys. Chem. Solids*, 1975, Vol. 36. pp. 315-320. Pergama Press. Printed in Great Britain
- [15] L. Yin, X. Zhan, K. Xu, F. Wang, Z. Wang, Y. Huang, Q. Wang, C. Jiang, J He, “Ultrahigh sensitive MoTe<sub>2</sub> phototransistors driven by carrier tunneling”, *Applied Physics Letters* 108, 043503 (2016)